CLOUD STATISTICS FROM SPACEBORNE BACKSCATTER LIDAR DATA ANALYSIS

Sébastien Berthier[1,2], Jacques Pelon[1], Patrick Chazette[2], Pierre Couvert[2], Geneviève Sèze[3] , François-Marie Bréon[2], Mathieu Lalande[3], Dave Winker[4] and Thierry Pain[5]

[1]*Service d'Aéronomie du CNRS, Institut Pierre-Simon-Laplace, Université Pierre-et-Marie-Curie, 4, Place Jussieu– 75252 Paris Cedex 05, France.*

[2]*Laboratoire des Sciences du Climat et de l'Environnement, Laboratoire mixte CEA-CNRS, F-91191 Gif-sur-Yvette, France.*

[3]*Laboratoire de Météorologie Dynamique, Institut Pierre-Simon-Laplace, Université Pierre et Marie Curie, 4, place Jussieu, – 75252 Paris Cedex 05, France.*

[4]Langley Research Center, NASA, Hampton, Virgina, USA.

[5]*ALCATEL Space, Cannes, France.*

ABSTRACT

The LITE spaceborne lidar database is used to revisit the analysis of cloud structural parameters. For this purpose, a specific algorithm has been developed to better account for multilayer cloud structure. Probability density function of cloud layer top height has been determined. The methodology is presented and the results are discussed. Such an approach highlights the interest of the synergism between active and passive remote sensors for global scale measurements dedicated to climatic studies but also to chemistry transport models by the effect of clouds on photolytic rates.

1. INTRODUCTION

One of the important objectives of the current climate research programs is the understanding of the impact of clouds and aerosols on the global radiation budget. Indeed, clouds and aerosols have a significant influence on the Earth's radiative balance and induce various climatic feedbacks that are still not enough known [1] [2]. The spatial heterogeneity of cloud structures and their microphysical properties significantly contributes to the modulation of the earth energy budget [3]. Moreover, the surface flux distribution in longwave radiation is very sensitive to both the geometrical structures and altitudes of clouds. A better knowledge of the tri-dimensional distribution of cloud layers is then required to improve existing climatic models.
New systems including spaceborne backscatter lidar systems are presently under development to give new insight in the vertical distribution of clouds and aerosols in the atmosphere and to provide new information on variables required for a better understanding of radiative and dynamical processes linked to the climate change problem. They offer the opportunity to better determine the presence of optically thin targets as cirrus clouds.

However, in the case of lidar systems operated from space, atmospheric backscattered signals present a reduced signal to noise ratios (SNR) as compared to ground-based systems, and a specific processing needs to be applied to measured signals.
In this work, we have applied and adapted the algorithm developed by Chazette et al. [4] to assess the probability density function (PDF) of cloud layers top heights from LITE Lidar (In-space Technology Experiment) profiles. The methodology is first explained and the results based on all the LITE data are presented and discussed.

2. METHOD

The LITE data have been recorded on board the Space Shuttle Discovery during the mission STS-64 in September 1994 [5] and can be found on the web site http://www-lite.larc.nasa.gov.

Cloud structure requires to consider the cloud layer top and bottom heights. Indeed, we have focused here on cloud top height as not influenced by the multiple scattering due to both the cloud density and the lidar solid angle. A specific inversion method has been developed to ensure the determination of the cloud top height. This method is based on the preliminary filtering of the range corrected lidar signal by calculating its variance in running-altitude windows first applied to individual vertical lidar profiles (Fig. 1). The range corrected lidar signal takes into account the switching of gain between day- and night-time operation, and the wavelength used (here 532 nm) [6]. The vertical profile of the relative variance of the signal S_f is calculated on a shot to shot basis using an adapting filtering window. After this first step, a threshold value S_T , estimated after statistical analysis on S_f, is applied to the variance profile obtained in order to identify the

scattering layers and their boundaries. We generate thus a binary state matrix of detection.

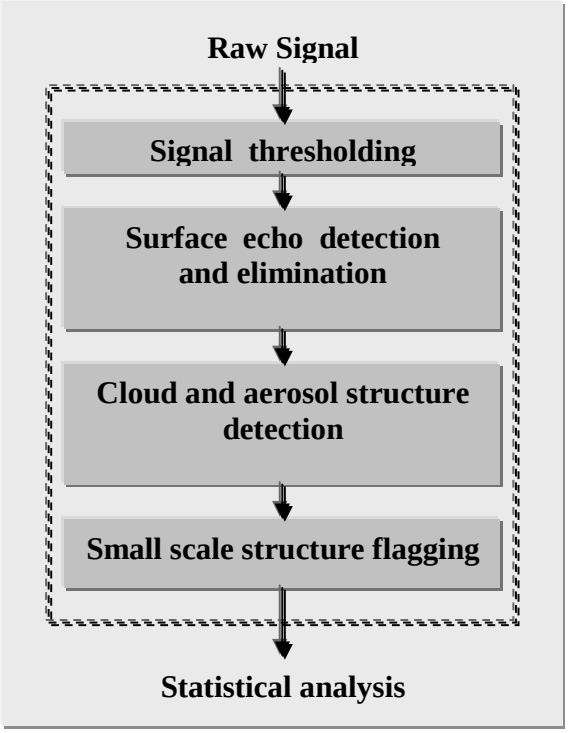

Fig. 1. Flow chart of the method.

A sensitivity study has been made on orbit 84. Two factors strongly influence the quality of the detection : the value of the threshold value S_T, and the type of filter used to test the occurrence of small isolated structures (with depth < 150m –10 points- on the vertical and 1400m –three shots- on the horizontal), that could be attributed to noise.

Two types of filters are studied : a median filter (hereafter defined as MF) and a second filter selecting structures with reference to nearby profiles (defined as NF). The distribution of small geometrical structures rejected by filter MF and NF are reported in fig. 2 and fig. 3, respectively, according to the threshold value. The NF filter appears to reject less structures than the MF filter. We note also that whatever the filter type, and for thresholds larger than 30, the rejected structures are principally located between the surface and 4km height. This could be due to presence of aerosol at this altitude range on the orbit 84. The number of rejected structures is rapidly increasing at middle and high altitudes as the threshold is decreased, which is mostly due to false alarm detection. For a threshold value of 10, the number of rejected points is thus multiplied by 2 and 4, for the MF and NF, respectively.

The determined value of cloud fraction may thus strongly depend on the detection of such structures and their classification into clouds or their rejection. Indeed, it is important to know the distribution of small structure in presence of clear sky. Given the two filter types, the statistics of rejected points are reported in figures 4 (MF) and 5 (AF). By comparison with the MF filter, the NF filter gives a factor of 10 less in the number of structure detected in presence of clear sky (no other feature is detected, but multiple isolated structures can be). Moreover, the number of structures detected is more uniformly distributed for the NF filter. Aerosol structures appear to be detected for large threshold values. The total number of rejected points is here again seen to stabilize for thresholds over 30. For this value the clear air fraction is 10.4 % using MF filter and 8.6 % for NF filter, assuming all flagged structures in clear air are removed from the statistics. If they are included into the statistics into the clear air part, the fraction is changed to 14.1 and 10.1 %, respectively.

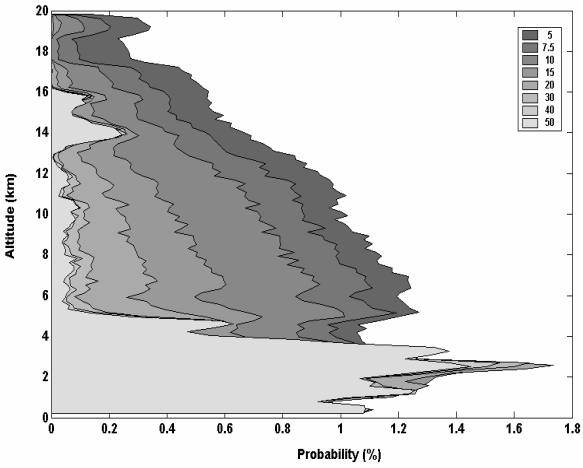

Fig. 2. Distribution of LITE small structures with median filter with threshold strength.

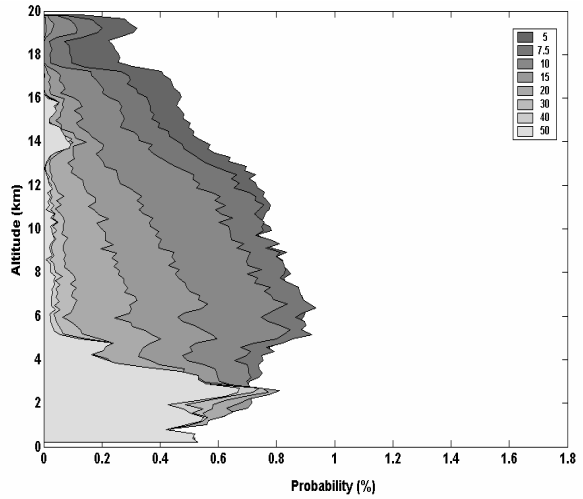

Fig. 3. Distribution of LITE small structures with new adjacent filter with threshold strength.

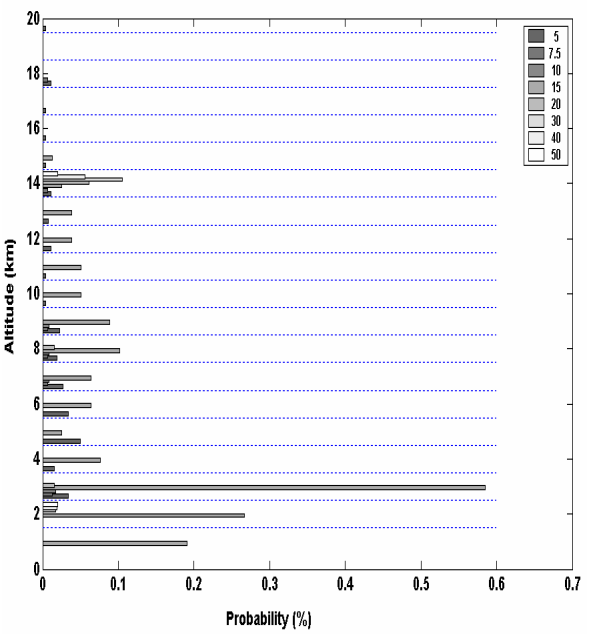

Fig. 4. Distribution of LITE small structures with MF filter in clear sky occurrence (normalized to the total number of flagged structures).

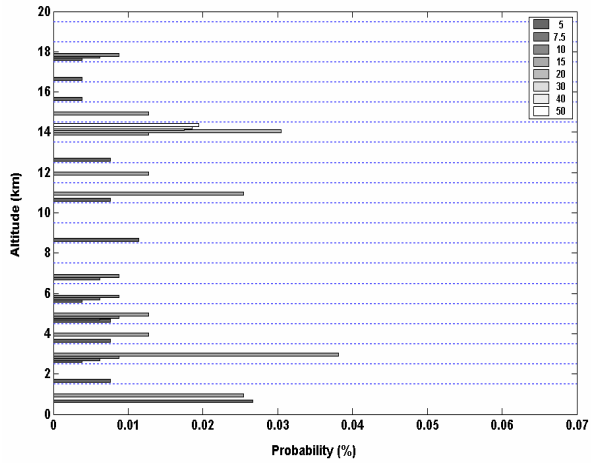

Fig. 5. Distribution of LITE small structures with NF filter in clear sky occurrence.

Further considering cloud detection, we have looked to the variation of the detected cloud fraction as a function of cloud structure (single or multiple layers of Low, Medium or High clouds) and threshold value. Results obtained after rejecting flagged structures are reported in Figure 6. It is shown that it is necessary to reach a threshold larger than 30, to reduce the variation in the detected cloud fraction. For lower values of the threshold, the low level clouds appear to be less detected, whereas the occurrence of detection of structures including multiple clouds rapidly increases. This is due to an increasing number of multiple noisy structures. A threshold value of 40 was thus selected for the analysis of cloud fraction at 532 nm.

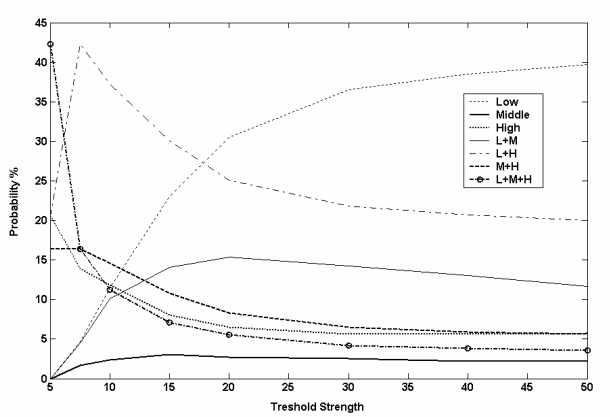

Fig. 6. Cloud fraction after filtering (NF filter) as a function of threshold.

3. RESULTS

A representative PDF considering the entire LITE data base has been obtained with the parameters defined in the previous analysis. Fig. 7 presents the occurrence histogram of all determined top cloud layers altitudes as a function of altitude in 15 m bins for wavelength 532 nm for the MF filter. In this figure, it is possible to distinguish three regions with sharp transition corresponding to a marked discontinuity in the layer top altitude statistics. Region **I** included both low and middle cloud classes of the ISCCP classification.
Although possibly biased due to the opacity of elevated cloud layers, the region I shows that a large amount of low clouds is detected.

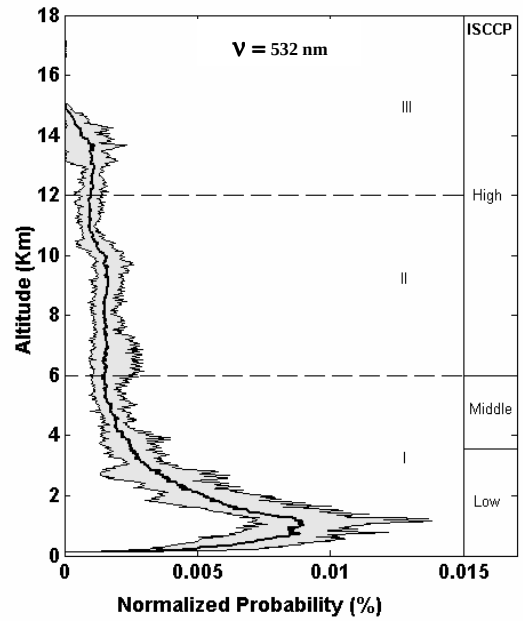

Fig. 7. Vertical distribution of cloud top height from LITE data at 532nm.

The high clouds are represented by the two sub-regions **II** and **III** separated by a sharp transition. Such a transition may be due to a discontinuity in the cloud top altitude between the denser clouds (cumulonimbus, cirrocumulus, and cirrostratus) and the semitransparent cirrus observed at different latitudes. The overall cloud fraction is 68 %. It is interesting to compare the shape of the cumulative PDF (CPDF) obtained from this set of data (Fig. 8) to previous results. Winker et al. (1998) [8] assess the CPDF only for the higher cloud layer top. A good agreement is observed up to an altitude of about 3 km. Here, we use all the retrieved cloud layers, including multiple-layer structures which explain the difference in the curves over 3 km height. The two curves are in good agreement with the statistics established by Warren et al (1985) which estimates to 40% the rate of low level clouds without any clouds above [9]. Each altitude range in Fig. 8 can be further referred to a specific cloud class identified in the ISCCP data base. CPDF retrieved from ISCCP daily means of data under the LITE footprint is also given in Fig. 8.

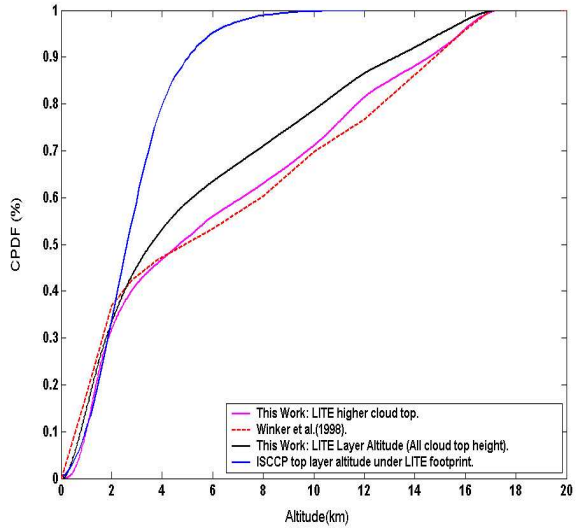

Fig. 8. Cumulative distribution of LITE and ISCCP cloud top height (ISCCP daily means).

4. CONCLUSION/PERSPECTIVES

A threshold algorithm has been applied to the analysis of LITE nighttime data in term of clouds statistics. The determination of the PDF of the cloud top height has been done on the entire database with a high spatial resolution (15 m in vertical resolution and 0.7 km along the ground track). This method allows to be flexible in terms of spatial resolution and allows sensitivity analysis to be done at high resolution. It allows to better evaluated the impact of detection algorithms on false alarm and no detection probabilities to accurately define cloud fraction and cloud statistics. Such an approach is developed to perform a sensitivity analysis in the perspective of the future CALIPSO mission [10].

REFERENCES

1. Arking A., The radiative effects of clouds an theirs impact on climate, *Bull. Am. Meteorol. Soc*., 71,795-813, 1991.

2. IPCC 2001. *Climate change 2000: The scientific basis contribution of working group I to the Third assessment report of the Intergovernmental Panel on Climate Change*, Cambridge University Press., Cambridge, United Kingdom and New York, 881 pp, 2001.

3. Melfi S.H., et al., Lidar Observations of the Vertically Organized Convection in the Planetary Boundary Layer over the Ocean, *J. Climate Appl. Meteo*r., 34,1092-1098, 1995.

4. Chazette P., et al., Determination by spaceborne backscatter lidar of the structural parameters of atmospheric scattering layers," *Appl. Op*t., 40, 3428-3440, 2001.

5. Winker D.M., et al., An overview of LITE: NASA's Lidar In Space Technology Experiment, *Proc. IEEE* 84, 164-180, 1996.

6. Osborn M.T., Calibration of LITE data, in *ILRC 19 th International Laser Radar Conferenc*e, Singh, U., Ismail, S., and Schwemmer, G. K. eds., NASA/CP-1998-207671/PT1, 245-247, 1998.

7. Rossow W.B., et al., ISCCP Cloud Data Products, *Bull. Amer. Meteor. Soc.*, 72, 2-20, 1991.

8. Winker D.M., Cloud Distribution Statistics from LITE, in *ILRC 19 th International Laser Radar Conferenc*e, Singh, U. N., Ismail, S., and Schwemmer, G. K. eds., NASA/CP-1998-207671/PT1, 955-958, 1998.

9. Warren S.G., Hahn, C.J. and London, J. Simultaneous occurrence of different cloud types, *J. Clim. Appl .Meteorol*., 24, 658-667, 1985.

10. Winker D. M., et al., The CALIPSO mission: Aerosols and cloud observations from space ", *Proc.* ILRC 21, Bissonnette, L., Roy, G., G.Vallee, Ed., pp. 735-738, 2000.